Development of a humidity estimation tool for automotive PEMFC stacks

Martin SERINE[a,b], Julie AUBRY[b], Zhixue ZHENG[a], Daniel HISSEL[a,c]

[a]Université Marie et Louis Pasteur, UTBM, CNRS, institut FEMTO-ST, FCLAB, F-90000, Belfort, France

[b]SYMBIO, St-Fons, France

[c]Institut Universitaire de France (IUF), Paris, France

ABSTRACT - Internal states knowledge of a proton exchange membrane fuel cell (PEMFC) is essential to enhance its performance level and further extend its lifespan. Real-time membrane water content estimation is crucial to prevent PEMFC from degrading conditions by avoiding drying or flooding. Estimating PEMFC humidity state can also contribute to establishing fault-tolerant control strategies. In this paper, a steady-state membrane water content estimation tool and a lumped cell voltage model have been developed. The cell voltage model has been validated using automotive fuel cell experimental data and compared with the outputs of a commercial simulation tool. The cell voltage value built on membrane water content estimation is sensitive to combined humidity and temperature variations, as validated by experimental data. This work paves the way for developing an online membrane water content observer for fault-tolerant control applications.

Keywords – Fuel cell, Diagnosis, Observer, Water content, Membrane, Drying, Flooding.

1. INTRODUCTION

In a context of greenhouse gas emission reduction in the transportation sector, the demand for sustainable mobility alternative solutions is growing worldwide. Electrical vehicles (EVs) market share has considerably increased over the last years. Within the European Union, planning to ban the sale of new petrol, diesel, and hybrid vehicles by 2035, the share of electric vehicles among new registrations for passenger cars has increased up to 14% in 2022 [1]. Even though most of them are powered by electrical batteries, this technology alone cannot address all customer needs, especially for heavy-duty transportation due to a certain number of limitations for intensive uses such as long-distance travel, payload and continuous operability. As a complementary solution to address these specific demands, Among those promising solutions, proton-exchange membrane fuel cells (PEMFC) systems offer a high-power density and reduced refueling time [2]. Their development has been initiated decades ago for specific applications. Since then, PEMFC embraces technological breakthrough in many fields such as materials, industrial processes but also control strategies [3].
PEMFC main technical improvements are driven by cost, efficiency and durability objectives. Reaching these objectives is crucial for industrial fuel cell manufacturers to enter the automotive market and meet the institutional targets [4]. A deep understanding of fuel cell technology and the underlying physics cannot be torn apart from cost reducing and lifespan increasing targets. Fuel cell are complex devices, entailing electrical, thermal, mechanical and electrochemical interactions at macro and microscales. Catching these complex phenomena is often impossible using in-situ measurements, hence the need of parameters called internal states.

Internal states, also called pivotal states, describe the physics inside an operating PEMFC, with a physical meaning [5]. Reactants partial pressure values, membrane water content and anode stoichiometry are the most studied internal states in the literature [5], [6], [7], [8]. Internal state observer is already used in several automotive engineering frameworks, such as battery State of Charge (SoC) estimation [9] or combustion torque estimation in internal combustion engines [10]. Among the conceivable internal states, PEMFC humidity level is crucial to enhance its performances and extend its lifespan. In fact, a well humidified membrane will be more conductive and induce less voltage losses [11]. Maintaining satisfying humidity level over time is also crucial to reduce fuel cell degradation. However, measuring a humidity level at system interfaces is difficult due to sensor costs and liquid water presence. It is often the case in operation, when vapor partial pressure is above saturation pressure for a given operating temperature. In-situ fuel cell water quantity measurement requires a very intrusive hardware and may be inaccurate in extreme operating conditions [12], [13], even if liquid water visualization experiments are useful to understand local phenomena [14]. Therefore, humidity observers have been widely studied over the last years, coupling accurate model and closed-loop control structures for model predicting control and diagnosis applications [15], [16]. PEMFC online diagnosis can also be performed without model [17], [18]. The next section is a state-of the art review of models for humidity state observation.

2. PEMFC MODELS FOR INTERNAL STATE ESTIMATION: A REVIEW

Estimating an unknown internal state tackles the question of model and control interactions. Modeling an operating PEMFC has garnered significant attention since the first fuel cell industrial applications [6], [7], [19]. PEMFC models' accuracy has considerably increased over the years, together with the global comprehension of complex physics associated. In the meantime, computation time has decreased due to microprocessors technology improvements, paving the way for even more complex simulations. Nonetheless, control applications require a high computational efficiency for the online implemented model. Building a fuel cell model is then a tradeoff to make between accuracy and computational efficiency. Fuel cell systems are subject to heat transfer, pressure drop, mechanical stress, degradation, electrical resistance, etc. Each sensitivity to operating conditions variations has a specific time constant, from a few milliseconds to hours. It is in the scope of the fuel cell model to account for this complexity, even in extreme operating conditions, to avoid degradation scenarios. PEMFC previous research has extensively investigated cell voltage modeling, which will be reviewed in the next subsection.

2.1. Cell voltage models

Cell voltage and stack humidity variations are often linked in stack operation. Besides, measuring stack voltage is necessary for fuel cell system level control purposes. Individual cell voltage measurement is also common in stack testing. Therefore it is relevant to build a robust cell voltage model and calibrate it

with test data. Modeling cell voltage involves considering reaction kinetics, ohmic losses, and mass transfer mechanisms. It is therefore necessary to put modeling work in accordance with real fuel cell physics. Although fuel cell voltage models are widespread in the literature, their formulation and structure may vary depending on the purpose and the complexity requested. An exhaustive review of fuel cell voltage models for thermal and water management strategies is provided by [20]. In most of the models described in the literature, cell voltage value is obtained by subtracting activation, ohmic and concentration losses from a reversible voltage [19]. However, the expression of thermodynamically reversible voltage may vary between the models, even though it results in a very slight variation within the PEMFC current density operating range.

Modeling PEM cell voltage using a lumped volume for anode and cathode is very common. Assuming a homogeneous temperature of these volumes and a uniform gas distribution among the channels, the cell voltage value can be derived from operating conditions with no spatial dependency. Such a model is very useful for control applications and within a given operating range. One of the most popular lumped cell voltage model has been developed by Pukrushpan et al. in 2004 [6] . This model has been derived under the assumption of isothermal PEMFC stack operation from Open Circuit Voltage (OCV) to maximum power operating point. The model is able to reproduce PEMFC stack transient response to operating conditions variations and is coupled with other sub models for membrane hydration or cathode pressure. It is still used in many recent modeling and control works. Another similar model considering isothermal stack operation has been proposed by Ritzberger et al. [21] in 2020 as an evolution of the one of Pukrushpan et al. [6]. More recently, fuel cell voltage models have been developed as part of observer building work. Chi et al. [7] derived a cell voltage model as part of a sliding mode observer. The authors stated to have only two fitting parameters to calibrate their model on real data. Kravos et al. [16] proposed a model qualified as "thermodynamically consistent" for observer applications. Under a realistic set of assumptions, a simplification of Butler-Volmer equations results in a sinus hyperbolicus function describing activation losses in cell voltage equation.

Despite their computational efficiency and relatively easy implementation, lumped models can not catch in-plane and through the membrane occurring phenomena. To overcome this limitation, 0D lumped model from Kravos et al. [16] has been enhanced with reactant depletion along the channel. The quasi 1D model can also distinguish two regions in the bipolar plates and Gas Diffusion Layer (GDL) interface. Doing so, Goshtasbi et al. [22] obtained a very accurate model, providing values distribution in every direction of the cell without compromising computational efficiency. The 1D-model through the membrane is solved twice, under the land and under the channel, then being also discretized along the channel to account for reactant depletion.

Finally, more complex cell voltage models exist in the literature, but their associated computational cost is an obstacle for online observer integration. Extracting a simple model from a multiphysics model framework is however possible [8]. The strong interaction between membrane hydration and cell voltage drives all the previously mentioned model structures. Real-time capable cell voltage models are often derived in a global modeling framework considering membrane hydration phenomena [6], [7], [16]. More recently, Gass et al. [23] developed a physics-based model, which is part of a global open-source model structure [24].

2.2. *Membrane hydration models*

As a product from oxidation-reduction equation inside the PEMFC, water cannot be torn apart from its underlying physics. As previously said, membrane hydration level strongly contributes to fuel cell performance. Proton Exchange Membranes (PEM) constitute the electrolyte of the fuel cell, enabling protons transport from anode to cathode side. They are also a support for catalyst layers. PEM are made of complex polymers with a backbone structure comparable to polytetrafluoroethylene (Teflon). Sulfonic acid chains are added, which enables protons to be transported in aqueous phase through hydronium complexes in flooded nano-scale pores [19]. Membrane water content, denoted by λ, relates the number of water molecules per sulfonic acid site in the membrane. At first sight, it might appear unrealistic to count molecules inside the pores. Experiments have however been led by Springer et al. [11] to correlate membrane water content to water activity. It consists in an isothermal sorption curve, given that water content evolution is proportional to polymer mass variation. The sorption curve cannot be found with measurement beyond saturation level (water activity equal to 1). At that point, water content values are close to 14 and remains constant. Bao et al. [25] gives an extrapolation of isothermal sorption curves with a sinus hyperbolicus expression, covering water activity values from 0 to 3. Despite their widespread use in the fuel cell modeling literature, correlations from Springer do not account for membrane structure and thickness evolution throughout the years. A more consistent and updated review about fuel cell polymers is provided by Kusoglu et al. [26].

The membrane water content values have no critical use itself, nevertheless it drives the ohmic losses of the fuel cell [19], and so its performances. Moreover, membrane water content appears in many water dynamics models. In fact, PEM are subjected to lots of phenomena through its thickness and at its interfaces. We distinguish two main contributors to water transport through the membrane, occurring in opposite directions. Firstly, electroosmotic drag is the transport of water molecules with the protons, from anode side to cathode side. One proton can literally drag up to 22 water molecules along with it [11]. Secondly, back diffusion is the diffusion process of water through the membrane. It is caused mainly by a concentration gradient, and therefore described by a Fick-like equation. The diffusion process is drived by water concentration gradient, then directed from cathode to anode in many cases. These transport mechanisms and their interactions with membrane water content are precisely described by Jiao et al. [27], and more recently by Gass et al. [28].

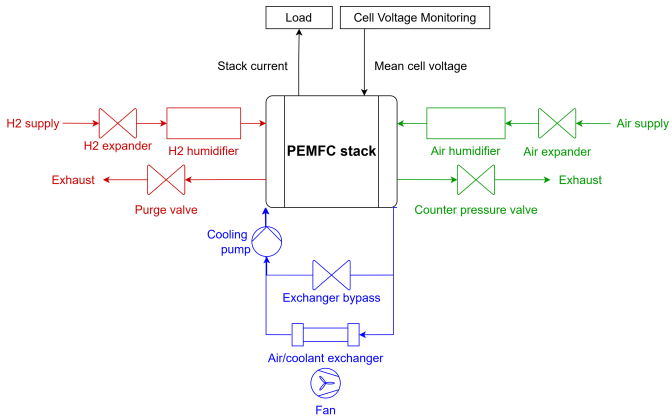

FIG. 1. Setup of a PEMFC stack under test.

3. CELL VOLTAGE MODEL

The main objective of the presented steady-state fuel cell voltage model is to make the link between its design parameters, the operating conditions and the measurable output performance of the stack. To do so, different sub models have been developed in Python code to provide robust and stable output towards operating conditions and fuel cell design parameter evolution.

In accordance with most of cell voltage models in the literature, cell voltage equation is written as a subtraction of va-

rious voltage losses from a reversible thermodynamical voltage [19][6]:

$$V_{cell} = E_{OC} - V_{act} - V_{ohmic} - V_{conc} \quad (1)$$

This section focuses on losses formulation and their contribution to the fuel cell voltage equation within the current density range of a typical polarization curve. Model output voltage values are compared with those of a commercial fuel cell model under the same calibration and with experimental data from an automotive stack.

TABLE 1. Symbols used for cell voltage model derivation.

Symbol	Description	Unit
E_{rev}	Reversible cell voltage	V
E_{OC}	Open Circuit potential	V
T	Stack temperature	K
j	Current density	A/cm²
j_0	Reference current density	A/cm²
$\alpha_{a,c}$	Charge transfer coefficient	–
λ	Membrane water content	–
n	Nb. of electrons exchanged	–
SR_{air,H_2}	Stoichiometric ratio	–
p_{H_2,O_2}	Reactants' partial pressures	bar
a_w	Water activity	–
$RH_{a,c,mem}$	Relative humidity	%
R	gas constant (8.314)	$J/mol \cdot kg$
F	Faraday constant (96485)	$s \cdot A/mol$
σ	Membrane conductivity	$(\Omega \cdot cm)^{-1}$
t_m	Membrane thickness	cm

3.1. Model assumptions

The following model equations have been selected under the following main hypotheses:

— **The model is steady-state.**
— There is **no liquid water in the fuel cell**. Water is only in the gaseous phase, even in the gas channels. Therefore, the Nernst reference potential value is $E^0 = 1.229$ V. Transient phenomena linked with water phase change and liquid water transport are not taken into account.
— Polymer **membrane thickness is constant**. Membrane swelling due to humidity variations is not taken into account.

3.2. Open Circuit Voltage (OCV)

E_{rev} is the reversible thermodynamically predictable voltage which varies with temperature and pressure. For a PEMFC consuming oxygen and hydrogen, and producing water, it can be written as:

$$E_{rev} = E^0 + \frac{\Delta\hat{s}}{nF}(T - T_0) + \frac{RT}{nF}\left[ln(p_{H_2}) + \frac{1}{2}ln(p_{O_2})\right] \quad (2)$$

where $\Delta\hat{s}$ is the entropy variation, $T_0 = 298.15$ K is the reference temperature, $n = 2$, and the other variables are defined in Table 1 .

Thus we can obtain the open-circuit equivalent potential:

$$E_{OC} = E_{rev} - OCV_{loss} \quad (3)$$

OCV_{loss} in (3) is a constant parameter, calibrated to fit the real OCV value which is gas crossover dependant.

3.3. Activation/kinetic losses

Activation losses are calculated using the Tafel equation, which is easier to solve in steady-state operation [20]:

$$V_{act} = \begin{cases} \frac{RT}{2F}\left(\frac{j}{j_0}\right), j \leq \frac{j_0}{1-\alpha_{a,c}} \\ \frac{RT}{2\alpha_{a,c}F} ln\left(\frac{j}{j_0}\right), j > \frac{j_0}{1-\alpha_{a,c}} \end{cases} \quad (4)$$

Activation voltage losses are calculated on both anode and cathode sides, then added together.

3.4. Concentration losses

Concentration losses occur mainly at high current density values. They are caused by diffusion processes and reactant transport limitations. As no mechanistic diffusion phenomena is included in the cell voltage model yet, the equation from O'Hayre [19] is used, and the value of j_{lim} is to be calibrated:

$$V_{conc} = \left(1 + \frac{1}{\alpha_c}\right)\left(\frac{RT}{2F}\right) ln\frac{j_{lim}}{j_{lim} - j} \quad (5)$$

Concentration voltage losses are calculated only on the cathode side.

3.5. Ohmic losses

Ohmic losses expression entails two main contributors, which are membrane resistance R_m and stack electrical resistance R_e. Thus, the overall ohmic voltage loss expression can be written as:

$$V_{ohmic} = (R_m + R_e)j \quad (6)$$

R_e is constant and part of the stack calibration. It represents the sum of all electrical resistances at component interfaces in the stack architecture.

R_m is the membrane ionic resistance, which is calculated according to Springer et al. [11]:

$$R_m = \int_0^{tm} \frac{dz}{\sigma(\lambda)} \quad in \quad \Omega \cdot cm^2 \quad (7)$$

σ is the membrane conductivity and is strongly dependant on membrane hydration state λ. t_m is the membrane thickness in cm, z is the coordinate fixed to the dry membrane. Under the assumption of constant membrane thickness, which correspond to no membrane swelling, we can simplify the membrane resistance equation:

$$R_m = \frac{t_m}{\sigma(\lambda)} \quad (8)$$

Springer et al. [11] were the first to establish a relationship between membrane conductivity and its water content λ. This expression is based on measurements made at 30°C with an additional temperature sensitivity:

$$\sigma_m = (b_{11}\lambda - b_{12})exp\left(b_2\left(\frac{1}{303} - \frac{1}{T}\right)\right) \quad in \quad (\Omega \cdot cm)^{-1} \quad (9)$$

b_{11}, b_{12}, b_2 are constant coefficients determined during the calibration process. They may vary based on the membrane material and cell configuration.

3.6. Cell voltage model validation

In this section, the previously derived model is compared to a commercial lumped cell voltage model, already validated by Symbio under a wide operating range. The same calibration of $OCV_{loss}, b_{11}, b_{12}, b_2, R_e$ is used. The commercial simulation tool has been used under the same assumptions to make sure

results can be compared. Additionally, the two models are evaluated using a dataset from a Symbio in-house designed full-size stack polarization curve. The same operating conditions are used as inputs for the two models. Comparative results are presented in Figure 2.

Operating conditions are the following ones:

— $P_{anode,in} = P_{cathode,in} = 2.5$ bar
— $SR_{air} = 1.8, \quad SR_{H_2} = 1.5$
— $T = 353.15$ K (using cooling loop regulation)
— $RH_{an,in} = 60\%, RH_{ca,in} = 35\%$

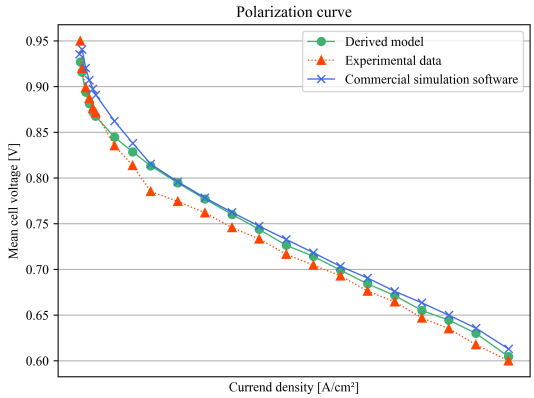

FIG. 2. Comparative results: polarization curve modeling.

The Mean Average Percentage Error (MAPE) has been used to assess the precision of the proposed model relative to the commercial simulation tool and experimental data. The MAPE indicator is calculated as:

$$MAPE = \frac{1}{n}\sum_{i=1}^{n}\left|\frac{y_i - \hat{y}_i}{y_i}\right| \times 100\% \tag{10}$$

with $\hat{y}_i$ being the voltage values obtained from the presented model, and y_i either the commercial simulation tool output or experimental values. The obtained MAPE values are given below:

— **Model versus Experimental data**: **1.38%**
— **Model versus Commercial simulation tool**: **1.23%**

These results tend to show that the presented model can reproduce the commercial simulation tool's results under the same operating conditions. Both derived and commercial simulation tool overestimate cell voltage value compared to experimental data, even though the MAPE indicator calculated using (10) is below 1.5%. The presented cell voltage model provides accurate results in steady-state mode. The next section will focus on membrane humidity modeling to make the link between operating conditions and membrane hydration state required for accurate cell voltage modeling.

4. HUMIDITY MODEL

4.1. *Model equations*

Under the assumption of no liquid water inside the PEMFC, we can obtain a simple relationship between membrane average water activity and its water content λ. In this work, we can assume $a_w = \frac{RH}{100}$, as $a_w \leq 1$. Therefore both indicators express the same humidity state and will be used without distinction in the next sections. Isothermal membrane sorption experiments have been carried out using the same protocol as Springer et al. [11]. Experimental data have been fitted to obtain a 5th order polynomial expression. The formula is only valid when a_w is less than 1:

$$\lambda(a_w) = \sum_{i=0}^{4} a_i {a_w}^i \tag{11}$$

a_i are empirical coefficients. In accordance with the model hypothesis of no liquid water, (11) has been extended for $a_w > 1$, using an equation form taken from Bao et al. [25] to obtain an equilibrium value of membrane water content:

$$\lambda_{eq}(a_w) = \frac{1}{2}\left[\sum_{i=0}^{4} a_i {a_w}^i\right](1 - \tanh(100[a_w - 1])) + \frac{1}{2}\left[\sum_{i=0}^{4} a_i + \left(14 - \sum_{i=0}^{4} a_i\right)(1 - \exp(-K(a_w - 1)))\right](1 + \tanh(100[a_w - 1])) \tag{12}$$

K is a shape factor to smooth the link between (11) and its extension (12). It has been chosen in accordance with the literature [25][28]. Coefficients $a_{0,1,2,3,4}$ are empirical.

4.2. *Model results*

Humidity and cell voltage submodels previously presented are coupled to obtain cell voltage results depending on operating conditions and consequently calculated membrane water content. We assume a constant RH value, equals to the average of the anodic and cathodic ones. Figure 3 presents cell architecture and related flows within a bipolar plate, and a stacked cell view with the PEM (Proton Exchange Membrane) in the middle. Anode and cathode are in counter flow, whereas coolant and cathode are in co-flow configuration.

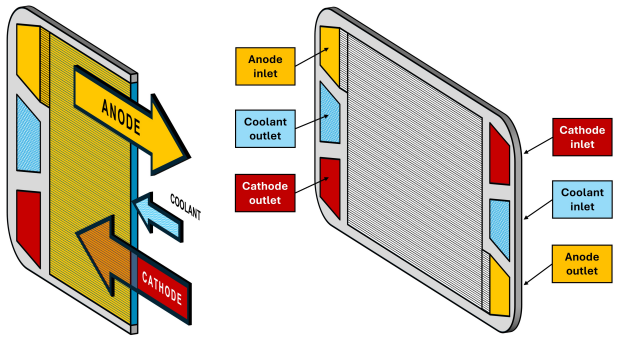

FIG. 3. Bipolar plate architecture and associated flows.

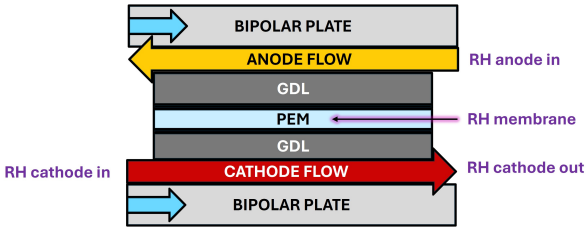

FIG. 4. Cell architecture (through-the-plane view) and associated RH values.

In steady-state operations, a membrane water content value for each operating point is calculated using (12). Then, cell voltage ohmic losses are obtained from (6). Figure 5 presents the obtained results for different operating conditions variations.

Figure 5 shows the sensitivity of the voltage ohmic losses model to operating conditions. The bar chart in blue represents the average relative humidity in the membrane, calculated under the previously mentionned hypothesis, and represented as *RH membrane* on Figure 4. Relative humidity values can be read on y-axis on the right. The green markers are modeled ohmic voltage

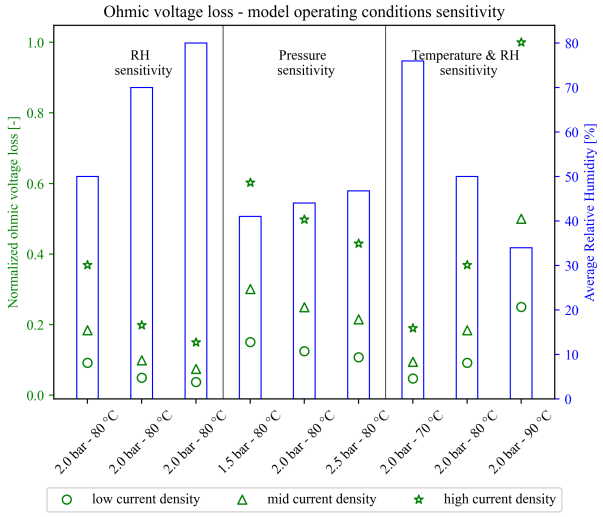

FIG. 5. Cell voltage ohmic losses operating conditions sensitivity.

losses. Their normalized values are displayed on y-axis on the left. As decribed in the presented cell voltage model, we can consider that ohmic voltage losses are prevalent in this range of current density values. Model sensitivity is divided in three parts, each containing three cases:

- For the RH sensitivity section corresponding to the three first data points, average RH is given as a model input value. We observe that ohmic voltage losses decrease as the RH increase at constant temperature and pressure conditions. This is in line with (11) in which λ is an increasing function of RH. Thus, conductivity values calculated from (9) decrease over increasing RH, resulting in a lower membrane resistance value. Ohmic voltage losses displayed on Figure 5 are calculated from (6). R_e being constant, even if R_m value is lower in humid conditions, ohmic losses increase linearily with current density.
- In the second part, only pressure values are varying. They are the same on anode and cathode side. Pressure variations have an impact on relative humidity. In fact, inlet relative humidity values are fixed, and the corresponding output values are calculated, taking into account the outlet pressure and considering constant pressure drop across the cell. Therefore, we can see in Figure 5 that average relative humidity values slighlty increase along with pressure. As a result, the same mechanism described in the previous part leads to a decrease in ohmic voltage losses.
- The last part of the sensitivity analysis combines RH and temperature within three selected operating points, that are representative of fuel cell operation. The same tendency as in previous parts is observed, considering that increasing operating temperature of the cell at a given inlet RH value will lead to a lower average humidity value and, therefore, increase ohmic voltage losses. The last case stands for a cell-drying scenario, in which combined high temperature and low relative humidity lead to a cell degradation mechanism. This case also highlights the need for the model to take into account the water produced by the electrochemical reaction within the fuel cell. In fact, the membrane is partially humidified by the water produced on the cathode side, and transported across the cell via a back diffusion mechanism.

To summarize, Figure 5 displays the model sensitivity to varying humidity, pressure, and temperature conditions. In accordance with equations from previous section, the humidity model is able to catch membrane conductivity variations with operating conditions.

5. EXPERIMENTAL DATA VALIDATION

The objective of this section is to compare model results with experimental data, and evaluate the model's ability to catch operating conditions variation in steady-state mode. To do so, a dataset from Symbio testing campaign is used. The global configuration of the stack under test is illustrated by Figure 1. There is no anodic recirculation, and both anode and cathode loops are humidified separately. The testing protocol consists in varying cooling loop regulated temperature, under constant pressure. The temperature sensitivity has been repeated for three current density levels (*Very low, Low and Mid*). Figure 6 displays the results. The bar chart in blue line corresponds to the minimum temperature in the stack cooling loop, its value can be read on y-axis on the left. The three current density levels are grouped on the x-axis on top of the figure. For each operating point, the previously derived model is used to:

- Calculate the average of anode inlet and cathode outlet relative humidity values, as presented in Figure 4.
- Use the humidity model to calculate a membrane water content value, and the cell voltage model to generate the corresponding voltage.
- Compare the obtained voltage value with the measured mean cell voltage on the testbench.

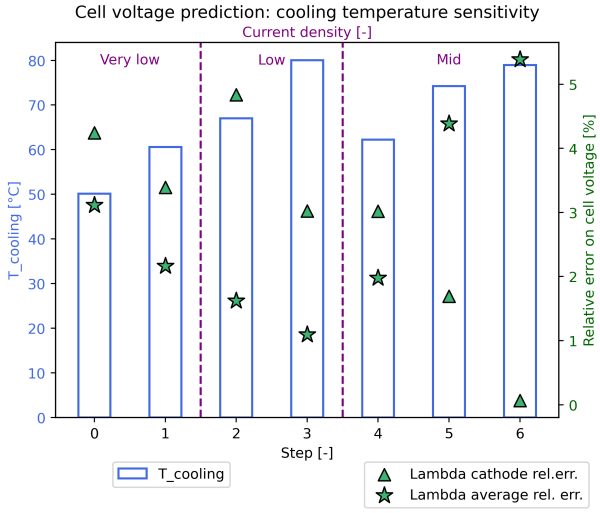

FIG. 6. Temperature sensitivity results and corresponding predicted voltage values, at a constant pressure.

Figure 6 displays the obtained relative error values on cell voltage prediction under two different hypothesis. The triangles and stars indicate the relative error in cell voltage using lambda cathode and lambda average, respectively. For the *Lambda average* serie, membrane water content is calculated considering as input an average RH value, displayed as *RH membrane* in Figure 4. For the *Lambda cathode* serie, membrane water content is calculated considering as input the theoretical cathode output RH value, displayed as *RH cathode out* in Figure 4. Considering the water produced on the cathode side, we know that *Lambda cathode* serie refers to more humid conditions. We observe that for all the operating points studied, relative error on cell voltage prediction is below 5.5%. At low current density, we observe that calculating a membrane water content value on average RH hypothesis provides better results than accounting for cathode outlet only. There is also a better prediction accuracy along with temperature. Average RH-based cell voltage error increases at mid current densities along with temperature, meaning that the humidity model could be further improved. Taking into account cathode outlet RH for cell voltage prediciton provides very arccurate results at high temperature and current density. Only ohmic voltage losses are displayed here, but activation losses cannot be neglected.

This results highlights the underestimation of membrane humidity under some operating conditions. Cell voltage prediction capability is limited by the membrane water content value in this model. Therefore, there is a need to model water transport through the membrane to obtain more accurate results.

6. CONCLUSIONS AND PERSPECTIVES

The presented cell voltage and humidity models link membrane hydration state and cell voltage in steady-state operations. The model, calibrated using experimental automotive PEMFC stack data, is able to catch operating conditions variations. In steady-state mode, the model can provide an accurate cell voltage value with less than 5.5% relative error towards temperature variations. Although this work paves the way for future real-time membrane water content observers, work is in progress to improve the humidity model. Typically, liquid water transport, phase change and transient regimes will be implemented. With these improvements, real-time observer will be implemented in PEMFC stack test benches.

7. ACKNOWLEDGEMENTS

This work has been supported by the European Union (Next Generation EU), the French State (France 2030, France Relance), the EIPHI Graduate School (contract ANR-17-EURE-0002) and the Region Bourgogne Franche-Comté.

8. RÉFÉRENCES

[1] Eurostat. Key figures on European transport – 2023 edition. 2023.

[2] Hussein Togun, Ali Basem, Tuqa Abdulrazzaq, Nirmalendu Biswas, Azher M. Abed, Jameel M. Dhabab, Anirban Chattopadhyay, Khalifa Slimi, Dipankar Paul, Praveen Barmavatu, and Amani Chrouda. Development and comparative analysis between battery electric vehicles (BEV) and fuel cell electric vehicles (FCEV). *Applied Energy*, 388 :125726, June 2025.

[3] Zikuo Liu, Shanshan Cai, Zhengkai Tu, and Siew Hwa Chan. Recent development in degradation mechanisms of proton exchange membrane fuel cells for vehicle applications : problems, progress, and perspectives. *Energy Storage and Saving*, 3(2) :106–152, June 2024.

[4] Clean Hydrogen Partnership. Clean Hydrogen JU SRIA - approved by GB - clean for publication (ID 13246486).

[5] Hao Yuan, Haifeng Dai, Xuezhe Wei, and Pingwen Ming. Model-based observers for internal states estimation and control of proton exchange membrane fuel cell system : A review. *Journal of Power Sources*, 468 :228376, August 2020.

[6] Jay T. Pukrushpan, Huei Peng, and Anna G. Stefanopoulou. Control-Oriented Modeling and Analysis for Automotive Fuel Cell Systems. *Journal of Dynamic Systems, Measurement, and Control*, 126(1) :14–25, March 2004.

[7] Xuncheng Chi, Fengxiang Chen, and Jieran Jiao. Model-based observer for vehicle proton exchange membrane fuel cell humidity based on adaptive sliding mode estimation technique. *International Journal of Hydrogen Energy*, 52 :750–766, January 2024.

[8] Maxime Piffard, Mathias Gerard, Ramon Da Fonseca, Paolo Massioni, and Eric Bideaux. Sliding mode observer for proton exchange membrane fuel cell : automotive application. *Journal of Power Sources*, 388 :71–77, June 2018.

[9] Jiahao Li, Joaquin Klee Barillas, Clemens Guenther, and Michael A. Danzer. A comparative study of state of charge estimation algorithms for LiFePO4 batteries used in electric vehicles. *Journal of Power Sources*, 230 :244–250, May 2013.

[10] Taixiong Zheng, Yu Zhang, Yongfu Li, and Lichen Shi. Real-time combustion torque estimation and dynamic misfire fault diagnosis in gasoline engine. *Mechanical Systems and Signal Processing*, 126 :521–535, July 2019.

[11] T. E. Springer, T. A. Zawodzinski, and S. Gottesfeld. Polymer Electrolyte Fuel Cell Model. *J. Electrochem. Soc.*, 138(8) :2334–2342, August 1991.

[12] Kuniyasu Ogawa, Tatsuyoshi Sasaki, Shigeki Yoneda, Kumiko Tsujinaka, and Ritsuko Asai. Two dimensional distribution measurement of electric current generated in a polymer electrolyte fuel cell using 49 NMR surface coils. *Magnetic Resonance Imaging*, 51 :163–172, September 2018.

[13] Kuniyasu Ogawa, Tatsuyoshi Sasaki, Shigeki Yoneda, Kumiko Tsujinaka, and Ritsuko Asai. Two-dimensional spatial distributions of the water content of the membrane electrode assembly and the electric current generated in a polymer electrolyte fuel cell measured by 49 nuclear magnetic resonance surface coils : Dependence on gas flow rate and relative humidity of supplied gases. *Journal of Power Sources*, 444 :227254, December 2019.

[14] Tim Dörenkamp, Mayank Sabharwal, Federica Marone, Felix N. Büchi, Thomas J. Schmidt, and Jens Eller. Investigation of Dynamic Water Cluster and Droplet Interactions in Polymer Electrolyte Fuel Cells using Operando X-ray Tomographic Microscopy. *J. Electrochem. Soc.*, 171(9) :094505, September 2024.

[15] Alireza Goshtasbi and Tulga Ersal. Degradation-conscious control for enhanced lifetime of automotive polymer electrolyte membrane fuel cells. *Journal of Power Sources*, 457 :227996, May 2020.

[16] Andraz Kravos, Daniel Ritzberger, Gregor Tavcar, Christoph Hametner, Stefan Jakubek, and Tomaz Katrasnik. Thermodynamically consistent reduced dimensionality electrochemical model for proton exchange membrane fuel cell performance modelling and control. *Journal of Power Sources*, 454 :227930, April 2020.

[17] J. Aubry, N. Yousfi Steiner, S. Morando, N. Zerhouni, and D. Hissel. Fuel cell diagnosis methods for embedded automotive applications. *Energy Reports*, 8 :6687–6706, November 2022.

[18] M. Ait Ziane, C. Join, M. Benne, C. Damour, N. Yousfi Steiner, and M.C. Pera. A new concept of water management diagnosis for a PEM fuel cell system. *Energy Conversion and Management*, 285 :116986, June 2023.

[19] Ryan P. O'Hayre, Suk-Won Cha, Whitney G. Colella, and F. B. Prinz. *Fuel cell fundamentals*. John Wiley & Sons Inc, Hoboken, New Jersey, third edition edition, 2016.

[20] Pedro Henrique Affonso Nóbrega. A review of physics-based low-temperature proton-exchange membrane fuel cell models for system-level water and thermal management studies. *Journal of Power Sources*, 558 :232585, February 2023.

[21] Daniel Ritzberger, Christoph Hametner, and Stefan Jakubek. A Real-Time Dynamic Fuel Cell System Simulation for Model-Based Diagnostics and Control : Validation on Real Driving Data. *Energies*, 13(12) :3148, June 2020.

[22] Alireza Goshtasbi, Benjamin L. Pence, Jixin Chen, Michael A. DeBolt, Chunmei Wang, James R. Waldecker, Shinichi Hirano, and Tulga Ersal. A Mathematical Model toward Real-Time Monitoring of Automotive PEM Fuel Cells. *Journal of The Electrochemical Society*, 167(2) :024518, January 2020.

[23] Raphaël Gass, Zhongliang Li, Rachid Outbib, Samir Jemei, and Daniel Hissel. An advanced 1D physics-based model for PEM hydrogen fuel cells with enhanced overvoltage prediction. *International Journal of Hydrogen Energy*, 97 :1108–1125, January 2025.

[24] Raphaël Gass, Zhongliang Li, Rachid Outbib, Samir Jemei, and Daniel Hissel. AlphaPEM : An open-source dynamic 1D physics-based PEM fuel cell model for embedded applications. *SoftwareX*, 29 :102002, February 2025.

[25] Cheng Bao and Wolfgang G. Bessler. Two-dimensional modeling of a polymer electrolyte membrane fuel cell with long flow channel. Part I. Model development. *Journal of Power Sources*, 275 :922–934, February 2015.

[26] Ahmet Kusoglu and Adam Z. Weber. New Insights into Perfluorinated Sulfonic-Acid Ionomers. *Chem. Rev.*, 117(3) :987–1104, February 2017.

[27] Kui Jiao and Xianguo Li. Water transport in polymer electrolyte membrane fuel cells. *Progress in Energy and Combustion Science*, 37(3) :221–291, June 2011.

[28] Raphaël Gass, Zhongliang Li, Rachid Outbib, Samir Jemei, and Daniel Hissel. A Critical Review of Proton Exchange Membrane Fuel Cells Matter Transports and Voltage Polarisation for Modelling. *Journal of The Electrochemical Society*, 171(3) :034511, March 2024.